Journal of Water Process Engineering 50 (2022) 103144

Contents lists available at ScienceDirect

Journal of Water Process Engineering

journal homepage: www.elsevier.com/locate/jwpe

Experiment and kinetic analysis of the effect of agitation speed on electrocoagulation process for the treatment of vinasse

Iqbal Syaichurrozi [a], Sarto Sarto [b,*], Wahyudi Budi Sediawan [b], Muslikhin Hidayat [b]

[a] Department of Chemical Engineering, Faculty of Engineering, University of Sultan Ageng Tirtayasa, Jl. Jendral Soedirman Km 3, Cilegon 42435, Indonesia
[b] Department of Chemical Engineering, Faculty of Engineering, Universitas Gadjah Mada, Jl. Grafika No.2, Yogyakarta 55281, Indonesia

ARTICLE INFO

Keywords:
Agitation speed
Electrocoagulation
Mechanistic model
Reynolds number
Vinasse

ABSTRACT

The electrocoagulation (EC) process was conducted to treat the vinasse waste with a variation of agitation speeds of 0, 250, and 500 rpm which can be expressed in Reynolds (Re) numbers of 0, 5.47×10^4, and 1.09×10^5, respectively. The goal of this study was to investigate the effect of agitation speed on the EC process, build a novel mechanistic model, and analyze the effect of agitation speed through the proposed mechanistic model. The measured parameters during the EC process were the changes in anode weight, electrical voltage, liquid temperature, liquid pH, liquid volume, COD concentration, Fe concentration, scum mass, and sludge mass. The results showed that the agitation of 250 rpm (Re of 5.47×10^4) resulted in a higher COD mass removal (67.62 %) than the two others. A detailed mechanistic model was successfully built with nine kinetic constants of k_a, N, k_v, k_f, k_{pH}, k_{Ri}, k_{Rd}, k_{ht}, k_c. Based on simulation results, various agitation speeds affected the values of N, k_v, k_f but not for the other kinetic constants. Furthermore, the equations expressing the values of N, k_v, k_f as a function of Re number were built. Finally, the optimization was conducted to find the optimum Re number resulting in the maximum COD mass removal. The predicted optimum Re number was 3.82×10^4 with COD mass removal of 70.01 % by the EC process for 8 h.

Nomenclatures

A_b	base area of EC reactor (dm^2)
A_e	active surface area of electrode (dm^2)
C_p	caloric capacity of solution (J/K)
d_a	diameter of agitator (dm)
F	Faraday's constant = 96,500C/mol
I	electrical current (A)
k_a	rate constant for adsorption (L/(mol.s)
k_c	rate constant for Newton's law of cooling (/s)
k_f	rate constant for flotation (/s)
k_h	rate constant for hydrolysis (L/(mol.s)
k_{ht}	rate constant for the increase in liquid temperature (L.K/(watt.s))
k_o	rate constant for oxidation (/s)
k_{pH}	rate constant for the changes in liquid pH (/s)
k_r	rate constant for reduction (/s)
k_{Rd}	rate constant for the decrease in resistance (dm.Ohm/(g.s))
k_{Ri}	rate constant for the increase in resistance (L.Ohm/(g.s))
k_v	constant rate for the changes in liquid volume (L/(g.s))
m	liquid mass (g)
m_{COD}	mass of *COD* (g)
$m_{Fe^{2+}}$	mass of Fe^{2+} (g)
m_{scum}	mass of *scum* (g)
m_{sludge}	mass of *sludge* (g)
M_{wCOD}	molecular weight of COD (g/mol)
M_{wFe}	molecular weight of Fe = 56 g/mol
M_{wH_2O}	molecular weight of H_2O = 18 g/mol
M_{ws}	molecular weight of sludge (g/mol)
N	amount of COD mol adsorbed by per mol Fe
n_{COD}	mol of *COD* (mol)
$n_{Fe^{2+}}$	mol of Fe^{2+} (mol)
n_{OH^-}	mol of OH^- (mol)
N_s	speed of agitator (rad/s)
n_{scum}	mol of *scum* (mol)
n_{sludge}	mol of *sludge* (mol)
pH	liquid pH
Q	energy (J)
R	electrical resistance (Ohm)
Re	Reynolds number

* Corresponding author.
E-mail address: sarto@ugm.ac.id (S. Sarto).

https://doi.org/10.1016/j.jwpe.2022.103144
Received 9 June 2022; Received in revised form 3 September 2022; Accepted 8 September 2022

t	electrolysis time (s)
T	liquid temperature (K)
T_o	surrounding temperature (K)
V	electrical voltage (V)
ν	volume of the waste (L)
ν_o	initial volume of vinasse (L)
w_e	width of the electrode (dm)
z	number of electron transfer for Fe = 2 or 3
ρ	liquid density (g/L)
ρ_{H_2O}	density of H_2O (g/L)
μ	liquid viscosity (g/(dm.s))
$[COD]$	molar of COD (mol/L)
$[Fe^{2+}]$	molar of Fe^{2+} (mol/L)
$[OH^-]$	molar of OH^- (mol/L)

1. Introduction

Electrocoagulation (EC), which is one of the wastewater treatments, can be applied to treat various wastewater [1–6]. EC utilizes the electrical current to do an electrolysis reaction. The anode and cathode are needed to connect the Direct Current (DC) or Alternating Current (AC) Power Supply to the liquid wastes, therefore, they have to be immersed in the wastes [2,4,7]. Anode and cathode are connected to the positive and negative poles of the DC power supply. One type of metal commonly used in EC as the anode and the cathode is iron (Fe) [2,8]. When the electrical current flows, the oxidation and reduction reactions occur at the anode and the cathode, respectively. In the oxidation reaction, the anode (Fe) is oxidized to either Fe^{2+} or Fe^{3+} ions, while in the reduction reaction, the water is reduced to OH^- ions and H_2 gas. Then, a chemical reaction between Fe^{2+} or Fe^{3+} ions and OH^- ions results in coagulants of $Fe(OH)_2$ or $Fe(OH)_3$ [2,9]. The coagulants adsorb pollutants to form flocs. The flocs are reacted to each other to form bigger flocs. Further, the bigger flocs will settle as sludge or be pushed by H_2 gas to the surface of the liquid as scum [4,10].

Based on the information above, the EC can change the concentration of pollutants and electrode-metal ions in wastewater and produce sludge and scum [3–5]. Commonly, the concentration of organic pollutants in wastewater is measured as the concentration of Chemical Oxygen Demand (COD) [11]. However, in detail, the EC also changes the liquid pH, liquid temperature, and liquid volume [12]. Therefore, the EC mechanism process is very complex. It is very interesting to model the EC process based on its mechanism process. Through modeling, the effect of affecting factors in the EC process can be studied clearly and deeply. The mechanistic models were successfully built by some previous studies. Syaichurrozi et al. [12] built a simple mechanistic model involving the changes in COD mass, sludge mass, and scum mass. Furthermore, a more detailed mechanistic model was built by Syaichurrozi et al. [13] by considering the changes in COD concentration, Fe concentration, sludge mass, and scum mass, but the liquid volume was assumed to be constant. Furthermore, Syaichurrozi et al. [14] modified the mechanistic model by considering the change in liquid volume, and then Syaichurrozi et al. [15] improved the mechanistic model by considering not only the change in liquid volume but also the changes in liquid pH and temperature. However, the profile of liquid volume, pH, and temperature during the EC process was approximated with the quadratic line as a function of time in those studies [14,15]. In order words, the kinetics of changes in the volume, pH and temperature of liquid were not built through the theoretical EC process mechanism. The summary of the mechanistic models from the previous studies is shown in Table 1. Therefore, the mechanistic model has to be improved in this study with the target shown in Table 1.

Vinasse is a liquid waste with a very high COD content [12,16]. Bioethanol industries release 8–20 L vinasse when producing 1 L bioethanol [16]. Due to its big volume and high COD content, vinasse is to be a serious liquid waste. Prior discharged to the environment, it has to be treated. One of the treatment methods, that can be utilized to treat the vinasse, is EC [13,14]. In Indonesia, the local vinasse contains a very high COD content (>100 g/L) [12]. Utilization of EC to treat the local vinasse has been conducted by our team. The application of EC to treat the local vinasse has been studied with variation of initial pHs (4.35, 5, 6) [13], variation of electrical voltages (7.5, 10, 12.5 V) [14], variation of electrical currents (2.5, 3, 3.5 A) [12]. Another factor, that is important in EC, is agitation speed [17–19]. Therefore, this study will investigate the effect of agitation speed on the EC process in treating the

Table 1
The mechanistic models developed by the previous studies and the target of this study.

Rate equation refers to:	[12]	[13]	[14]	[15]	The target of this study
$\frac{dFe}{dt}$	No	Yes	Yes	Yes	Yes
$\frac{dCOD}{dt}$	Yes	Yes	Yes	Yes	Yes
$\frac{dSludge}{dt}$	Yes	Yes	Yes	Yes	Yes
$\frac{dScum}{dt}$	Yes	Yes	Yes	Yes	Yes
$\frac{dv}{dt}$	No	No	Quadratic line $v = f(t)$	Quadratic line $v = f(t)$	Yes
$\frac{dpH}{dt}$	No	No	No	Quadratic line $pH = f(t)$	Yes
$\frac{dT}{dt}$	No	No	No	Quadratic line $T = f(t)$	Yes

Notes:
"Yes" means that the rate equation for the component is included in the mechanistic model.
"No" means that the rate equation for the component is not included in the mechanistic model.
"Quadratic line" means that the rate equation for the component is included in the mechanistic model, which is built using a quadratic line, not built based on the reaction mechanism.

Table 2
All equations included in the mechanistic model

Components	Equations
$\frac{dm_{Fe^{2+}}}{dt}$	$\frac{M_{wFe}I}{zF} - k_a\frac{m_{Fe^{2+}}m_{COD}}{v\,M_{wCOD}}$
$\frac{dm_{COD}}{dt}$	$-N\frac{k_a m_{Fe^{2+}}m_{COD}}{v\,M_{wFe}}$
$\frac{dm_{sludge}}{dt}$	$(M_{wFe}+N\,M_{wCOD})\frac{k_a m_{Fe^{2+}}m_{COD}}{v\,M_{wFe}\,M_{wCOD}} - k_f m_{sludge}$
$\frac{dm_{scum}}{dt}$	$k_f m_{sludge}$
$\frac{dv}{dt}$	$-\frac{2\frac{I}{zF}BM_{H_2O}}{\rho_{H_2O}} - k_v m_{scum}$
$\frac{d[OH^-]}{dt}$	$\frac{2\left(\frac{I}{zF} - k_a\frac{m_{Fe^{2+}}m_{COD}}{v\,M_{wFe}\,M_{wCOD}}\right) - [OH^-]\left(-\frac{2\frac{I}{zF}BM_{H_2O}}{\rho_{H_2O}} - k_v m_{scum}\right)}{v}$
$\frac{dpH}{dt}$	$k_{pH}(14-(-\log([OH^-])))$
$\frac{dV}{dt}$	$I\left(k_{Ri}\frac{m_{sludge}}{v} - k_{Rd}\frac{pH\,m_{Fe^{2+}}\left(l_e-\left(\frac{v_0-v}{A_b}\right)\right)w_e}{v}\right)$
$\frac{dT}{dt}$	$k_{ht}\frac{VI}{v} - k_c(T-T_o)$

local vinasse. This study was new in experiment and modeling in treating the vinasse by EC method at various agitation speeds. The aims of this study are (1) to study the effect of agitation speed on the EC process, (2) to build a detailed mechanistic model, and (3) to investigate the effect of agitation speed on the EC process quantitatively with the mechanistic model developed.

2. Mechanism of the EC process

All the reactions that occur during the EC process are assumed as chemical reactions with irreversible processes. During the EC process, the oxidation and reduction reactions occur at the anode and cathode, respectively [1,2]. In the oxidation reaction, the iron (Fe) is oxidized to Fe^{2+} ion (Eq. (1)). Many studies [13,14,20,21] proved that the product of the oxidation reaction at the iron anode is Fe^{2+} ion, not Fe^{3+} ion.

$$Fe\,(s) \xrightarrow{k_o} Fe^{2+}(aq) + 2\,e^- \tag{1}$$

In the reduction reaction, the water is reduced to OH^- ion and H_2 gas (Eq. (2)).

$$2\,H_2O\,(l) + 2\,e^- \xrightarrow{k_r} H_2(g) + 2\,OH^-(aq) \tag{2}$$

Furthermore, the Fe^{2+} ions react with OH^- ions to form coagulants of $Fe(OH)_2$ [1,2] (Eq. (3), hydrolysis reaction). The $Fe(OH)_3$ can also be produced from the Fe^{2+} ion when the liquid contains high dissolved oxygen [1], but the vinasse contains a very low dissolved oxygen [22]. Therefore, this study assumed that the type of coagulant produced in the liquid during the EC process was $Fe(OH)_2$.

$$Fe^{2+}(aq) + 2\,OH^-(aq) \xrightarrow{k_h} Fe(OH)_2\,(s) \tag{3}$$

Furthermore, the $Fe(OH)_2$ adsorbs pollutants. Assuming that every mol $Fe(OH)_2$ can adsorb "N" mol of COD to form flocs, then the flocs react with each other to form bigger flocs which then settle to sludge as shown in Eq. (4a).

$$Fe(OH)_2\,(s) + N\,COD\,(aq) \xrightarrow{k_a} sludge\,(s) \tag{4a}$$

It is assumed that k_a is a second-order reaction rate constant that is not affected by the total mol of $Fe(OH)_2$ and COD in the reaction shown in Eq. (4a). Because of spontaneous hydrolysis of Fe^{2+} to the coagulants, the rate-determining step is the generation of Fe^{2+} electrolytically [23], for simplifying, Eq. (4a) can be modified to Eq. (4b).

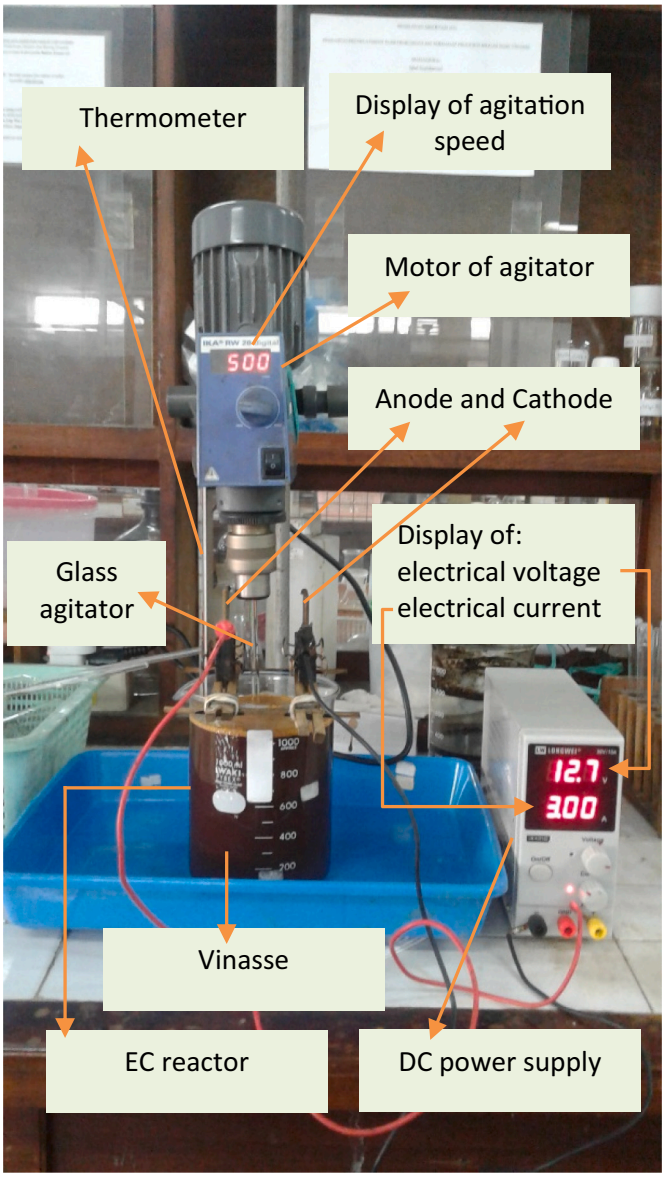

Fig. 1. Experimental set-up of laboratory-scale EC process.

$$Fe^{2+}\,(aq) + N\,COD\,(aq) \xrightarrow{k_a} sludge\,(s) \tag{4b}$$

The sludge can be separated by sedimentation. However, a part of sludge can go up as scum due to flotation by evolved H_2 during the EC process (Eq. (5)) [13].

$$Sludge\,(s) \xrightarrow{k_f} Scum\,(s) \tag{5}$$

3. Modeling

The mechanistic model is built based on the chemical process given in Eqs. (1)–(5).

3.1. Net production rate of Fe^{2+} mass

The production rate of Fe^{2+} mol by oxidation reaction follows the Faraday's law [14] (Eq. (6)).

$$\frac{dn_{Fe^{2+}}}{dt} = \frac{I}{zF} \tag{6}$$

Table 3
Experimental data.

Time (s)	Anode weight loss (g)	Voltage (V)	T (K)	pH	Volume (mL)	COD		Fe		Scum (g)	Sludge (g)
						g/L	g	g/L	g		
Agitation speed of 0 rpm											
0	0	12.6	301.65	4.1	1000.00	113.70	113.70	0.11	0.11	0.00	0.00
3600	–	8.8	314.15	4.5	985.75	105.19	103.69	–	–	0.23	–
7200	–	8.1	318.65	4.7	966.76	108.37	104.77	1.90	1.84	0.59	12.89
10,800	–	7.9	320.15	5	938.26	105.19	98.69	–	–	1.29	–
14,400	–	8.2	321.65	5.4	905.02	104.82	94.86	3.37	3.05	3.96	24.48
18,000	–	8.7	322.65	5.9	824.28	106.80	88.04	–	–	10.70	–
21,600	–	9.4	325.15	6.4	724.54	106.80	77.38	3.77	2.73	19.22	33.27
25,200	–	11	330.15	6.4	582.07	93.05	54.16	–	–	34.14	–
28,800	24.94	12.4	333.65	6.2	468.08	88.82	41.57	5.88	2.75	51.94	42.62
Agitation speed of 250 rpm											
0	0	12.3	300.65	4.1	1000.00	113.70	113.70	0.11	0.11	0.00	0.00
3600	–	9.1	316.65	4.5	995.25	106.60	106.09	–	–	0.32	–
7200	–	8.5	320.15	4.8	976.25	110.15	107.53	3.06	2.99	0.48	9.08
10,800	–	8.5	321.15	5.2	947.76	105.71	100.19	–	–	0.97	–
14,400	–	8.6	323.15	5.7	886.02	108.37	96.02	4.27	3.78	4.12	22.42
18,000	–	9	324.65	6.3	791.03	108.37	85.73	–	–	13.35	–
21,600	–	10	327.15	6.7	705.55	102.16	72.08	3.03	2.14	24.23	34.17
25,200	–	11.8	332.15	6.7	563.07	94.16	53.02	–	–	39.51	–
28,800	24.60	13.6	338.65	6.7	406.34	90.61	36.82	5.18	2.10	61.09	38.87
Agitation speed of 500 rpm											
0	0	12.4	300.65	4.1	1000.00	113.70	113.70	0.11	0.11	0.00	0.00
3600	–	9.2	316.15	4.5	995.67	104.82	104.37	–	–	0.21	–
7200	–	8.3	320.15	4.7	982.69	110.15	108.24	2.51	2.47	0.34	9.02
10,800	–	8.3	321.15	5.1	961.05	108.37	104.15	–	–	0.51	–
14,400	–	8.1	321.65	5.4	926.44	108.37	100.40	2.95	2.73	0.75	22.46
18,000	–	8.5	322.15	5.8	887.49	109.26	96.97	–	–	1.95	–
21,600	–	8.7	323.65	6.4	839.89	108.37	91.02	3.50	2.94	5.36	33.30
25,200	–	9.6	325.15	6.9	774.98	108.37	83.99	–	–	10.32	–
28,800	24.71	10.2	328.65	7	697.09	94.16	65.64	4.60	3.20	18.56	51.48

The consumption rate of Fe^{2+} mol by adsorbing the COD is written in Eq. (7).

$$\frac{dn_{Fe^{2+}}}{dt} = -k_a[Fe^{2+}][COD]v \tag{7}$$

Hence, the net production rate of Fe^{2+} mol is shown in Eq. (8).

$$\frac{\mathrm{dn_{Fe^{2+}}}}{\mathrm{dt}} = \frac{\mathrm{I}}{\mathrm{zF}} - \mathrm{k_a}[\mathrm{Fe^{2+}}][\mathrm{COD}]\mathrm{v}$$

$$\frac{dn_{Fe^{2+}}}{dt} = \frac{I}{zF} - k_a\frac{n_{Fe^{2+}}n_{COD}}{v} \tag{8}$$

Therefore, the production rate of Fe^{2+} mass is shown in Eq. (9_.

$$\frac{dm_{Fe^{2+}}}{dt} = \frac{M_{wFe}I}{zF} - k_a\frac{m_{Fe^{2+}}m_{COD}}{v\,M_{wCOD}} \tag{9}$$

3.2. Net consumption rate of COD mass

The net consumption rate of COD mol is shown in Eq. (10).

$$\frac{dn_{COD}}{dt} = -N\frac{k_a n_{Fe^{2+}}n_{COD}}{v} \tag{10}$$

Therefore, the net consumption rate of COD mass is shown in Eq. (11).

$$\frac{dm_{COD}}{dt} = -N\frac{k_a m_{Fe^{2+}}m_{COD}}{v\,M_{wFe}} \tag{11}$$

3.3. Net production rate of sludge mass

The production rate of sludge mass can be expressed through Eq. (12).

$$\frac{\mathrm{dn_{sludge}}}{\mathrm{dt}} = \frac{\mathrm{k_a n_{Fe^{2+}} n_{COD}}}{\mathrm{v}}$$

$$\frac{dn_{sludge}}{dt} = \frac{k_a m_{Fe^{2+}}m_{COD}}{v\,M_{wFe}\,M_{wCOD}} \tag{12}$$

Based on Eq. (4b), the sludge can be expressed as Fe-$(COD)_N$. Therefore, the molecular weight of sludge can be written in Eq. (13).

$$M_{ws} = M_{wFe} + N\,M_{wCOD} \tag{13}$$

Hence, Eq. (12) is modified to Eq. (14).

$$\frac{dm_{sludge}}{\mathrm{dt}} = (M_{wFe} + N\,M_{wCOD})\frac{k_a m_{Fe^{2+}}m_{COD}}{v\,M_{wFe}\,M_{wCOD}} \tag{14}$$

The consumption rate of sludge mass due to flotation can be written in Eq. (15).

$$\frac{dm_{sludge}}{dt} = -k_f m_{sludge} \tag{15}$$

The net production rate of sludge mass can be written in Eq. (16).

$$\frac{dm_{sludge}}{dt} = (M_{wFe} + N\,M_{wCOD})\frac{k_a m_{Fe^{2+}}m_{COD}}{v\,M_{wFe}\,M_{wCOD}} - k_f m_{sludge} \tag{16}$$

3.4. Net production rate of scum mass

The net production rate of scum mass is expressed in Eq. (17).

$$\frac{dm_{scum}}{dt} = k_f m_{sludge} \tag{17}$$

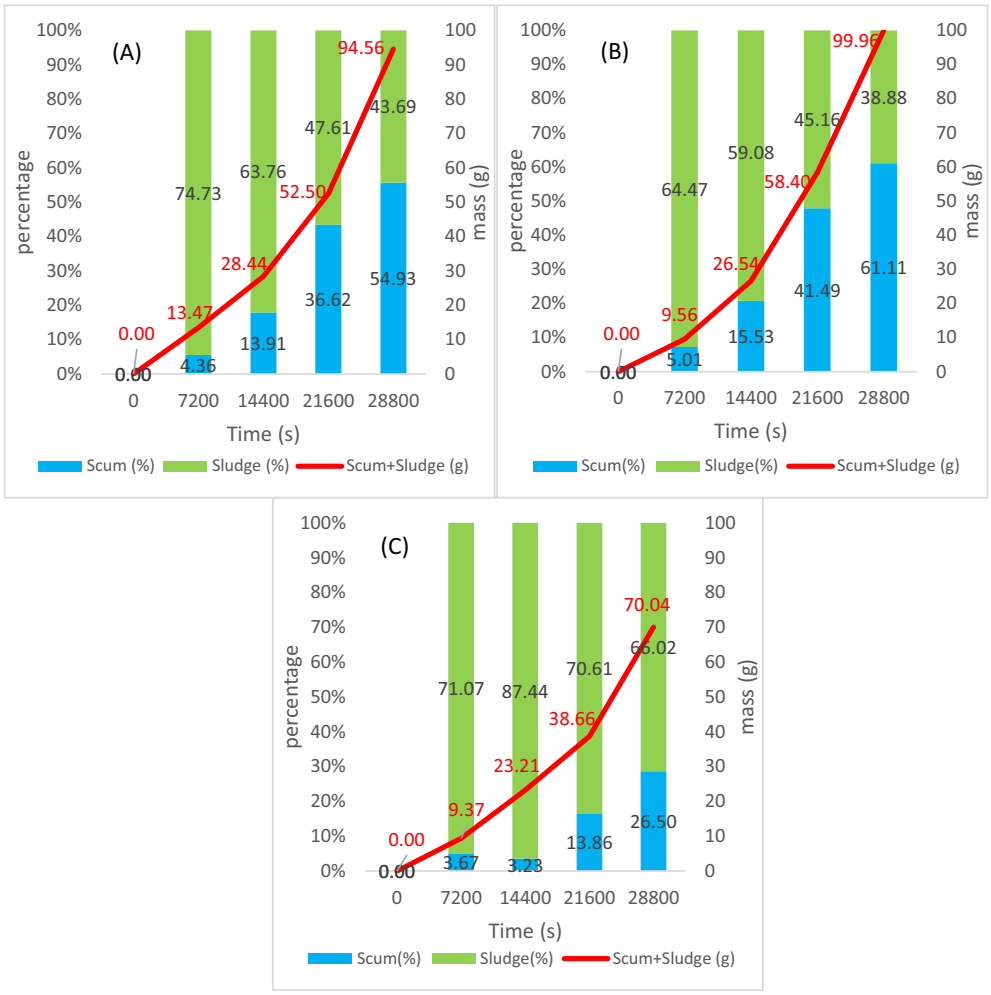

Fig. 2. Profiles of scum and sludge productions at (A) 0 rpm, (B) 250 rpm, (C) 500 rpm.

3.5. Reduction rate of liquid volume

During the EC process, the liquid volume decreases as a function of time. A decrease in liquid volume can be caused by (1) reduction reaction Eq. (2) and (2) scum production [14].

The decrease in liquid volume due to the reduction reaction can be written in Eq. (18).

$$\frac{dv}{dt} = -\frac{2\frac{I}{zF}M_{wH_2O}}{\rho_{H_2O}} \tag{18}$$

The decrease in liquid volume due to the scum production is written in Eq. (19).

$$\frac{dv}{dt} = -k_v m_{scum} \tag{19}$$

Hence, the complete equation for the reduction rate of liquid volume is shown in Eq. (20).

$$\frac{dv}{dt} = -\frac{2\frac{I}{zF}M_{wH_2O}}{\rho_{H_2O}} - k_v m_{scum} \tag{20}$$

3.6. The changes in pH

Based on Eqs. (1)–(3), the net production rate of OH^- ion mol is twice as much as the net production rate of Fe^{2+} ion mol. Therefore, the net production rate of OH^- ion mol is shown in Eq. (21).

$$\frac{dn_{OH^-}}{dt} = 2\frac{dn_{Fe^{2+}}}{dt}$$

$$\frac{dn_{OH^-}}{dt} = 2\left(\frac{I}{zF} - k_a\frac{n_{Fe^{2+}}n_{COD}}{v}\right)$$

$$\frac{dn_{OH^-}}{dt} = 2\left(\frac{I}{zF} - k_a\frac{m_{Fe^{2+}}m_{COD}}{v\,M_{wFe}\,M_{wCOD}}\right) \tag{21}$$

Furthermore, Eq. (21) is modified to Eq. (22).

$$\frac{d[OH^-]v}{dt} = 2\left(\frac{I}{zF} - k_a\frac{m_{Fe^{2+}}m_{COD}}{v\,M_{wFe}\,M_{wCOD}}\right)$$

$$v\frac{d[OH^-]}{dt} + [OH^-]\frac{dv}{dt} = 2\left(\frac{I}{zF} - k_a\frac{m_{Fe^{2+}}m_{COD}}{v\,M_{wFe}\,M_{wCOD}}\right)$$

$$\frac{d[OH^-]}{dt} = \frac{2\left(\frac{I}{zF} - k_{a_v}\frac{m_{Fe^{2+}}m_{COD}}{M_{wFe}\,M_{wCOD}}\right) - [OH^-]\frac{dv}{dt}}{v} \tag{22}$$

Furthermore, the liquid pH can be calculated through Eq. (23).

$$\frac{dpH}{dt} = k_{pH}(14 - (-log([OH^-]))) \tag{23}$$

3.7. The changes in voltage

A correlation between electrical voltage, current, and resistance is

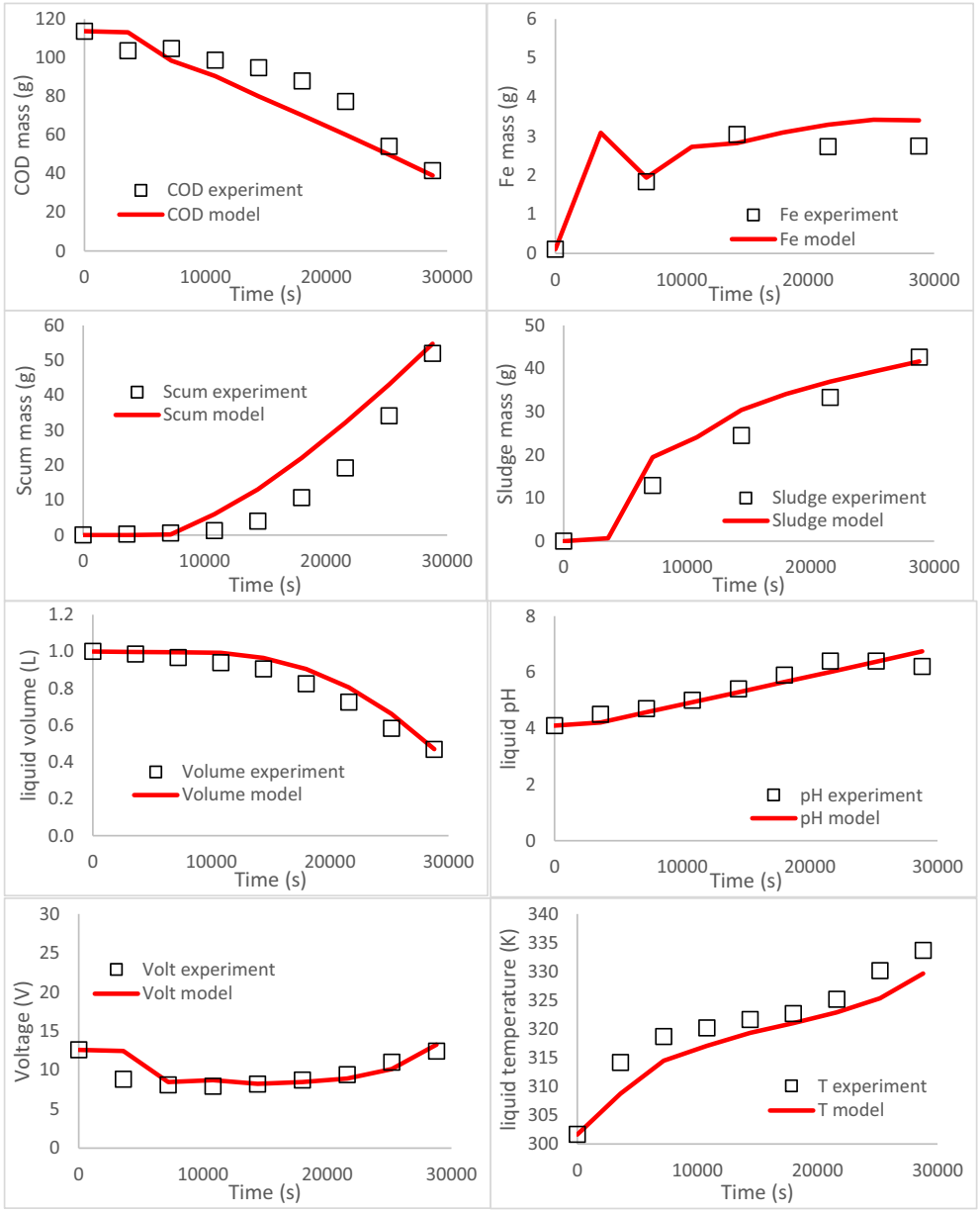

Fig. 3. Simulation results for agitation speed of 0 rpm (Re 0).

shown in Eq. (24) [14].

$$V = IR \tag{24}$$

For I = constant, Eq. (24) is modified to Eq. (25).

$$\frac{dV}{dt} = I\frac{dR}{dt} \tag{25}$$

The electrical resistance has a straight relationship with the sludge concentration. Furthermore, it has a reverse relationship with the Fe^{2+} concentration, pH, and surface area of the electrode. Hence, it can be written through Eq. (26).

$$\frac{dR}{dt} = k_{Ri}\left(\frac{m_{sludge}}{v}\right) - k_{Rd}\left(pH\left(\frac{m_{Fe^{2+}}}{v}\right)A_e\right) \tag{26}$$

Hence,

$$\frac{dV}{dt} = I\left(k_{Ri}\frac{m_{sludge}}{v} - k_{Rd}\frac{pH\ m_{Fe^{2+}}\ A_e}{v}\right)$$

$$\frac{dV}{dt} = I\left(k_{Ri}\frac{m_{sludge}}{v} - k_{Rd}\frac{pH\ m_{Fe^{2+}}\left(l_e - \left(\frac{v_0 - v}{A_b}\right)\right)w_e}{v}\right) \tag{27}$$

3.8. The changes in liquid temperature

During the EC process, the energy supplied to the liquid can be predicted by Eq. (28) [14].

$$\frac{dQ}{dt} = VI \tag{28}$$

Thus, the energy supplied to the liquid increases the liquid temperature (Eq. (29)) [24,25].

$$\frac{dQ}{dt} = m\ c_p\ \frac{dT}{dt} \tag{29}$$

Substituting Eq. (28) to Eq. (29) to get Eq. (30).

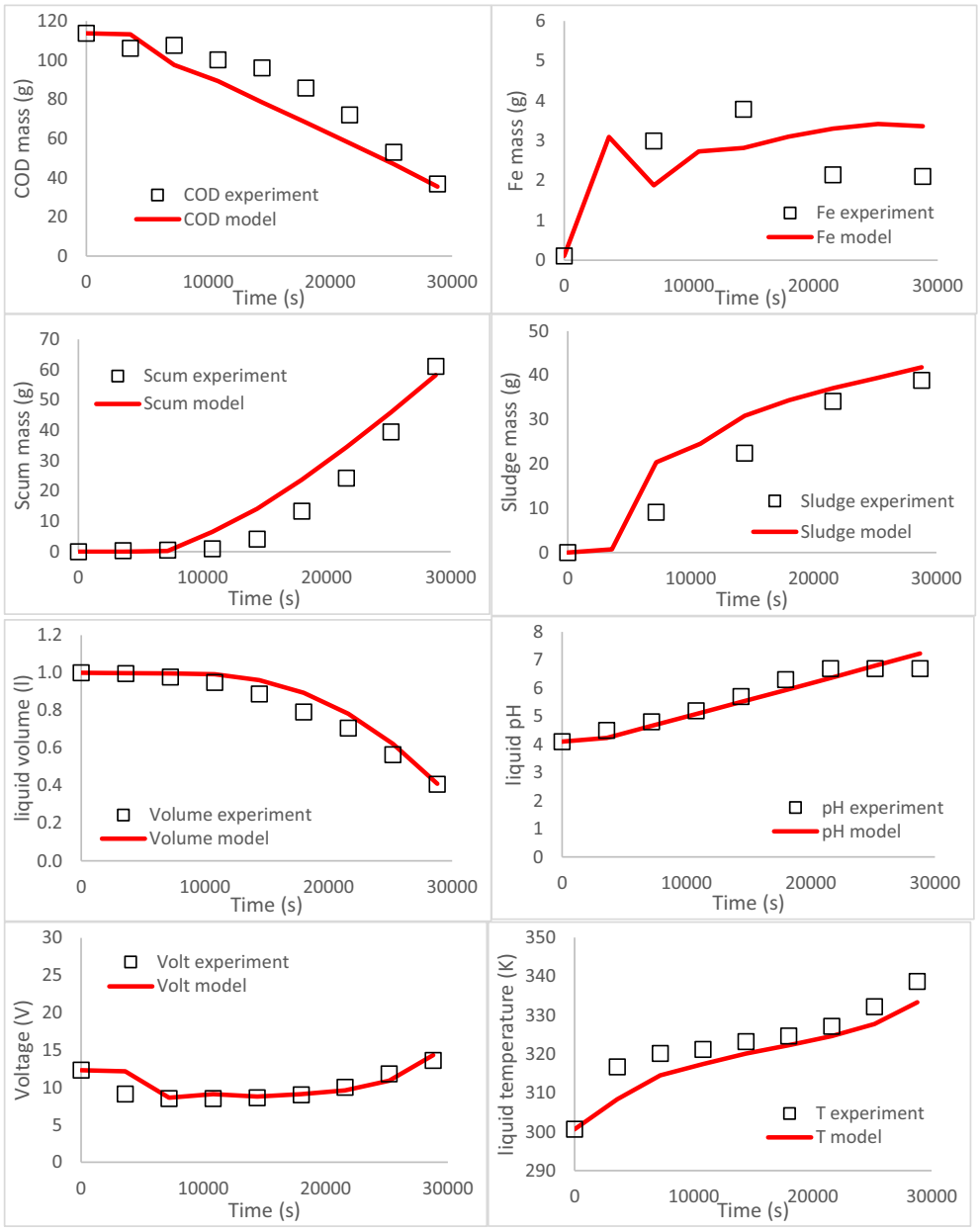

Fig. 4. Simulation results for agitation speed of 250 rpm (Re 7.35×10^4).

$$\frac{dT}{dt} = \frac{VI}{m\, c_p} \tag{30}$$

The energy loss to the surroundings is assumed to follow the Newton's law of cooling [26] written in Eq. (31).

$$\frac{dT}{dt} = -k_c(T - T_o) \tag{31}$$

The total net energy supplied to the liquid can be written in Eq. (32).

$$\frac{\mathrm{dT}}{\mathrm{dt}} = \frac{\mathrm{VI}}{\mathrm{m\, c_p}} - \mathrm{k_c(T - T_o)}$$

$$\frac{dT}{dt} = \frac{VI}{v\, \rho\, c_p} - k_c(T - T_o) \tag{32}$$

For simplifying, the ρ and c_p are assumed to be constant during the EC process, so Eq. (32) is modified to Eq. (33) with $k_{ht} = \frac{1}{\rho\, c_p}$.

$$\frac{dT}{dt} = k_{ht}\frac{VI}{v} - k_c(T - T_o) \tag{33}$$

All equations included in the mechanistic model are presented in Table 2.

4. Materials and methods

4.1. Local vinasse

Local vinasse was obtained from one of the bioethanol industries in Indonesia. The waste has COD of 113.70 g/L, total Fe of 0.11 g/L, and pH of 4.1. The density and viscosity of the vinasse are 1036.34 g/L and 0.1392 g/(dm.s), respectively.

4.2. Experimental set-up

EC reactor was built from 1 L-beaker glass (cylinder shape) with

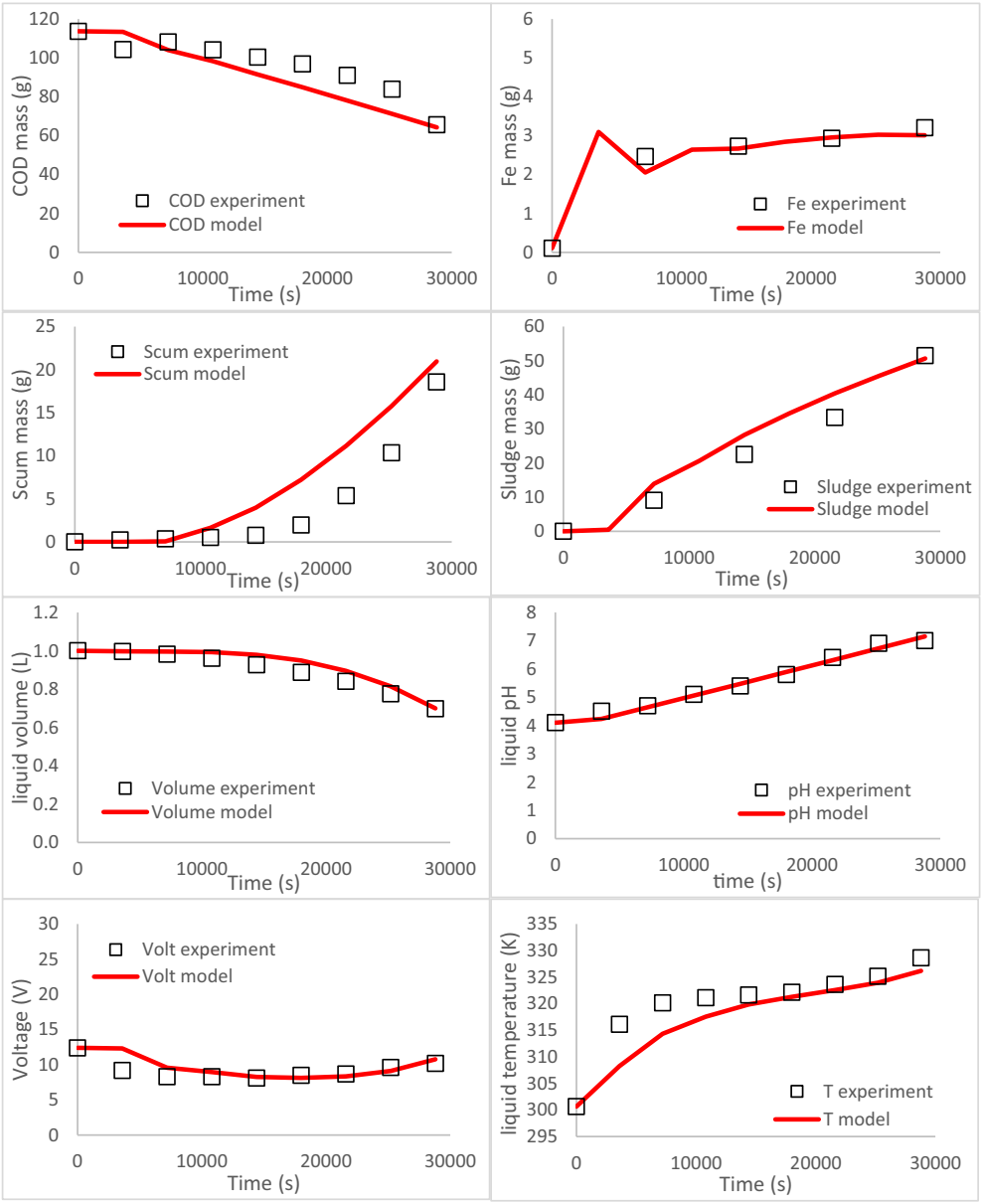

Fig. 5. Simulation results for agitation speed of 500 rpm (Re 1.47×10^5).

outer diameter, inner diameter, and height of 1.1 dm, 1.05 dm, and 1.52 dm, respectively. The experimental set-up of this study followed the previous studies of [13,14]. The irons (Fe) were used as electrodes having length, width, and thickness of 2 dm, 0.3 dm, and 0.03 dm, respectively. The anode and cathode were placed vertically at a distance of 0.55 dm. The vinasse volume in the EC reactor was 1 L. The active electrode dimension of length, width, and thickness was 0.95 dm, 0.3 dm, and 0.03 dm, respectively. The glass agitator with impeller length and width of 0.53 dm and 0.06 dm, respectively. A DC power supply (Long Wei, Series of LW-K3010D, 0–30 V, 0–10 A) was used as an electrical source. The experimental set-up of the laboratory-scale EC process is shown in Fig. 1.

4.3. Experimental design and procedures

Before used in the EC process, the anode and cathode were immersed in HCl 5%*v*/v for 15 min, then they were rinsed using the distilled water. After that, they were dried using the oven at a mercury temperature of 105–110 °C for 2 h and then weighed. The clean anode and cathode were placed vertically at a distance of 0.55 dm in the EC reactor containing 1 L of vinasse. The anode and cathode were connected to the positive and negative poles of the DC power supply. The EC process was run under the batch system for 8 h with a constant electrical current of 3A. The agitation speed was varied to be 0, 250, and 500 rpm. During the process, per 1 h, the changes in electrical voltage, liquid temperature, liquid pH, and surface liquid height were measured. The liquid temperature and pH were measured by using a mercury temperature and a digital pH meter. The scum produced on the liquid surface was taken by using a plastic spoon, and then dried in the oven with a temperature of 105–110 °C for at least 2 h and weighed. Meanwhile, the liquid sample of ±10 mL was taken and placed in reaction tubes for settling for 24 h. The supernatants formed in the tubes were taken for the COD and total Fe analyses. The COD analysis was conducted through the open reflux and titration method of SNI 06-6989.15-2004. The total Fe in the solution was measured using Atomic Absorption Spectroscopy (AAS). After the EC process, the anode was rinsed using distilled water, dried in the oven, and weighed. The sludge mass was measured using a method proposed in a previous study of [14]. The experiments in this study were

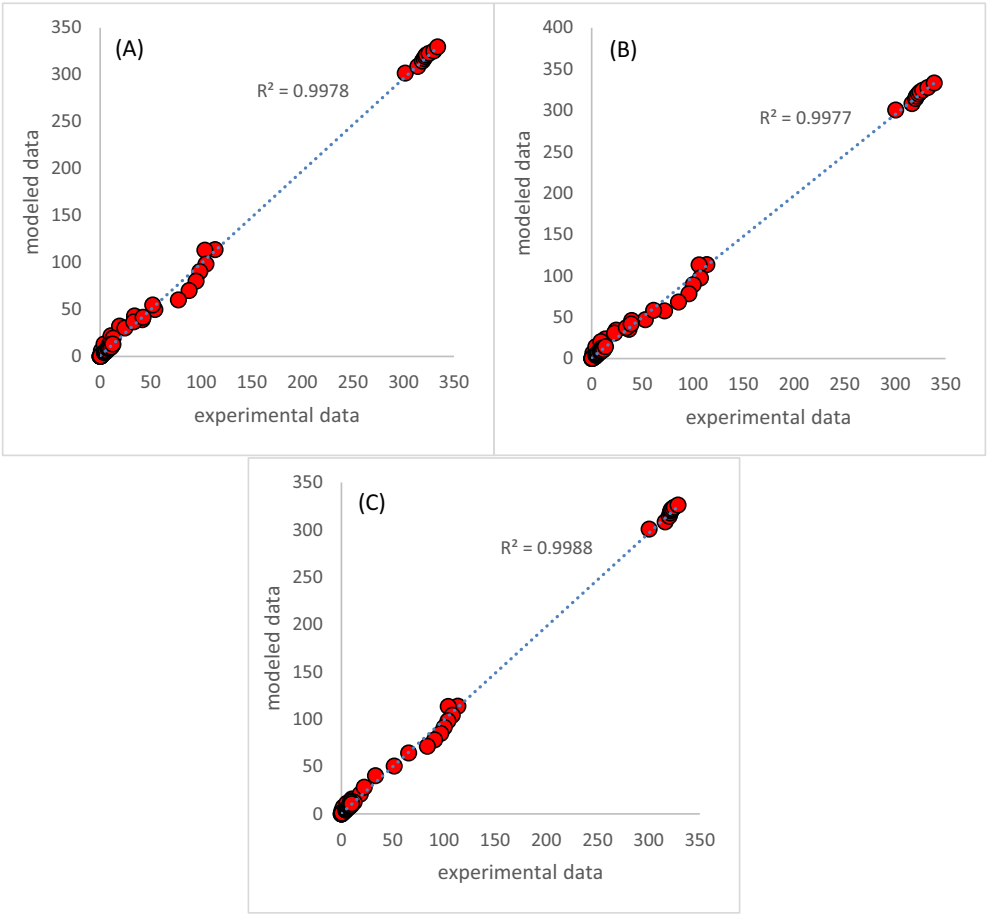

Fig. 6. Correlation between the experimental data and the modeled data at (A) 0 rpm, (B) 250 rpm, and (C) 500 rpm.

Table 4
Kinetic constant results

Constants	Unit	Agitation speed			Mean	SD	RSD (%)	Judgment
		0 rpm (Re 0)	250 rpm (Re 5.47×10^4)	500 rpm (Re 1.09×10^5)				
k_a	L/(mol.s)	1.09×10^{-4}	1.10×10^{-4}	1.06×10^{-4}	1.08×10^{-4}	2.33×10^{-6}	2	Not affected by Re
N	–	6.00	6.28	3.90	5.39	1.30	24	Affected by Re
k_v	L/(g.s)	1.22×10^{-6}	1.27×10^{-6}	1.98×10^{-6}	1.49×10^{-6}	4.24×10^{-7}	28	Affected by Re
k_f	/s	8.22×10^{-5}	8.62×10^{-5}	3.17×10^{-5}	6.67×10^{-5}	3.04×10^{-5}	46	Affected by Re
k_{pH}	/s	7.71×10^{-6}	9.12×10^{-6}	8.92×10^{-6}	8.58×10^{-6}	7.62×10^{-7}	9	Not affected by Re
k_{Ri}	L.Ohm/(g.s)	1.44×10^{-5}	1.33×10^{-5}	9.54×10^{-6}	1.24×10^{-5}	2.53×10^{-6}	20	Not affected by Re
k_{Rd}	dm.Ohm/(g.s)	1.02×10^{-4}	9.06×10^{-5}	6.93×10^{-5}	8.74×10^{-5}	1.67×10^{-5}	19	Not affected by Re
k_{ht}	L.K/(watt.s)	5.02×10^{-5}	5.44×10^{-5}	5.32×10^{-5}	5.26×10^{-5}	2.16×10^{-6}	4	Not affected by Re
k_c	/s	5.00×10^{-5}	5.28×10^{-5}	5.63×10^{-5}	5.30×10^{-5}	3.15×10^{-6}	6	Not affected by Re

conducted without replication. The process control was EC process without agitation (agitation speed 0 rpm).

This study studied the effect of the agitation speeds of 0, 250, and 500 rpm. For generalization, the agitation speed (rpm) was changed to be the Reynolds (Re) number with Eq. (34) [27]. For simplification, the density and viscosity of the vinasse are assumed constant during the EC process.

$$Re = \frac{\rho N_s {d_a}^2}{\mu} \tag{34}$$

By using Eq. (34), the agitation speed of 0, 250, and 500 rpm was equal to Re of 0, 5.47×10^4, and 1.09×10^5, respectively.

4.4. Kinetic analysis

The measured data obtained during the experiment were COD concentration, total Fe concentration, scum mass, sludge mass, electrical voltage, liquid temperature, liquid pH, and liquid volume per 1 h. A curve fitting between experimental data and modeled data was graphed. The deviation of those two was calculated using a Sum of Squares of Errors (SSE) (Eq. (35)).

$$(\mathrm{SSE}) = \sum_{i=1}^{n} (experimental\ data - modeled\ data)^2 \tag{35}$$

The adjustable kinetic constants in the mechanistic model are k_a, N, k_v, k_f, k_{pH}, k_{Ri}, k_{Rd}, k_{ht}, k_c. The values of the kinetic constants are obtained by minimizing the SSE value with help of Ms. Excel.

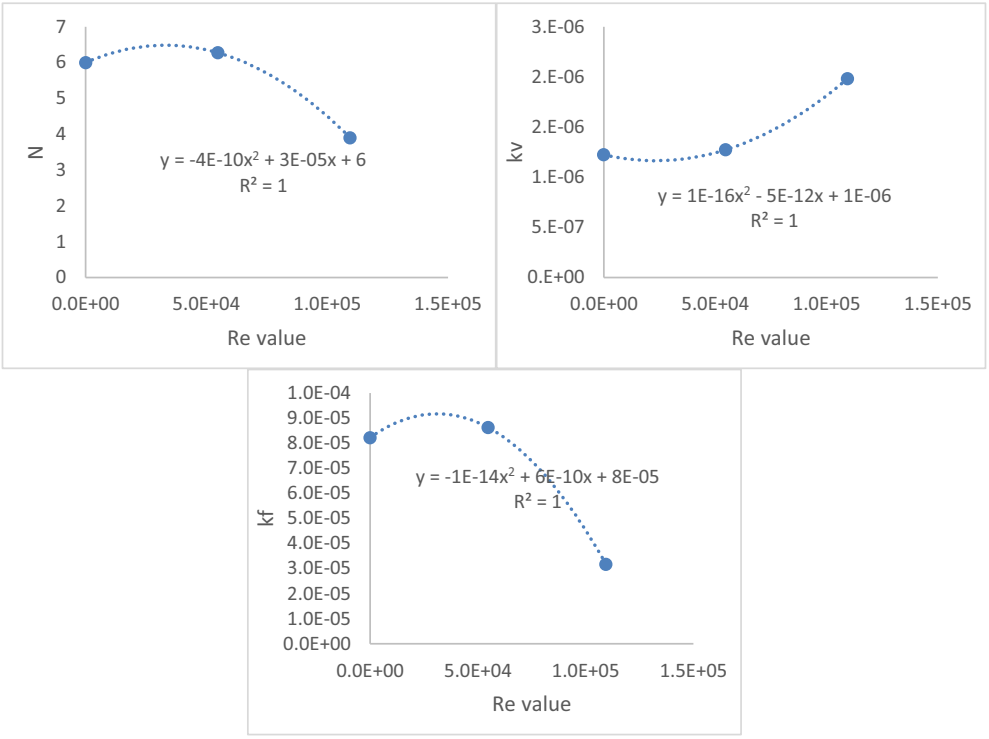

Fig. 7. Correlation between the Re number and the value of N, k_v, k_f.

5. Results and discussion

5.1. Experimental data

The EC process at various agitation speeds was successfully conducted and the experimental data were shown in Table 3. The experimental data in this study included anode weight loss (g), electrical voltage (V), liquid temperature (K), liquid pH, liquid volume (mL), COD concentration (g/L), total Fe concentration (g/L), scum mass (g), and sludge mass (g).

5.1.1. Anode, Fe, COD mass profiles

The anode weight decreased due to the oxidation of anode (iron) to Fe^{2+}. In this study, the electrical current was maintained constant at a value of 3 A. The anode weight loss can be predicted through Eq. (36).

$$anode\ weight\ loss\ (g) = \frac{M_{wFe} I t}{zF} \tag{36}$$

where $M_{wFe} = 56$ g/mol; $I = 3$ A; $z = 2$; $F = 96{,}500$C/mol; $t =$ time in second.

By using Eq. (36), the value of anode weight loss was predicted to be 25.07 g. Experimentally, the anode weight loss in this study was almost the same as the prediction which was 24.60–24.94 g (Table 3). If the $z = 3$, the value of anode weight loss was predicted to be 16.71 g. Therefore, it confirmed that the correct z value was 2 and the product of the oxidation reaction of Fe was Fe^{2+}, not Fe^{3+}. The agitation speed (Re number) did not affect the anode weight loss because based on Eq. (36), the anode weight loss was just affected by electrical current and electrolysis time.

The remaining Fe mass in liquid is shown in Table 3. The remaining Fe mass in the liquid was around 8.51–12.91 % or the Fe mass involved in coagulant formation was around 87.09–91.49 %. The COD mass in the solution is also shown in Table 3. The COD mass decreased from the beginning until the end of the process. The coagulants adsorbed the COD to form sludge. The COD mass removal for 0, 250, and 500 rpm was 63.44, 67.62, and 42.27 %, respectively. Based on these values, an agitation speed of 250 rpm (Re of 5.47×10^4) resulted in a better COD mass removal than the others. A lower and a higher than the agitation speed of 250 rpm, the EC process was not effective.

A previous study reported that electrooxidation of organic pollutants in wastewater occurs when the wastewater contains a high chloride concentration (about 40 g/L) [28]. The oxidation process occurs because chloride (Cl^-) in liquid turns into chlorine (Cl_2) at the anode. Furthermore, the Cl_2 reacts with H_2O to form hypochlorous acid (HOCl) and hypochlorite ion (OCl^-). Under acidic conditions, the concentration of hypochlorous acid is more dominant than the hypochlorite ion. Furthermore, the hypochlorous acid has a stronger oxidizing power than the hypochlorite ion, so organic pollutants are easily oxidized at acidic pH. However, this study used the local vinasse with a very low chloride concentration (about 1.1 g/L) [12]. Therefore, the decrease in COD concentration in this study was caused by the adsorption by the coagulant, not by the oxidation by hypochlorous acid.

5.1.2. Sludge and scum mass profiles

Sludge and scum production at various agitation speeds during the EC process are shown in Table 3 and Fig. 2. After the EC process for 8 h, the total mass of sludge and scum produced at agitation speeds of 0, 250, 500 rpm was 94.56, 99.96, and 70.04 g, respectively (Fig. 2). The agitation speed of 250 rpm resulted in a more total mass of sludge and scum than the others. It means that the adsorption process of COD on the coagulants at 250 rpm was more effective than the other agitation speeds. In more detail, the percentage of scum mass increased while the percentage of sludge mass decreased during the EC process at all various agitation speeds (Fig. 2). The final percentage ratios (after 8 h) of scum: sludge at 0, 250, and 500 rpm was 54.93:45.07, 61.11:38.89, and 26.50:73.50, respectively. The percentage of scum mass (54.93 %) at 0 rpm was lower than that at 250 rpm (61.11 %) because the adsorption process occurred effectively and resulted in much more flocs at 250 rpm than that at 0 rpm, so the flocs at 250 rpm were easier to be pushed on the liquid surface by H_2 gas than another. Meanwhile, the scum mass at 500 rpm (26.50 %) was lower than that at 250 rpm (61.11 %) because too high agitation speed caused the contact time between coagulants

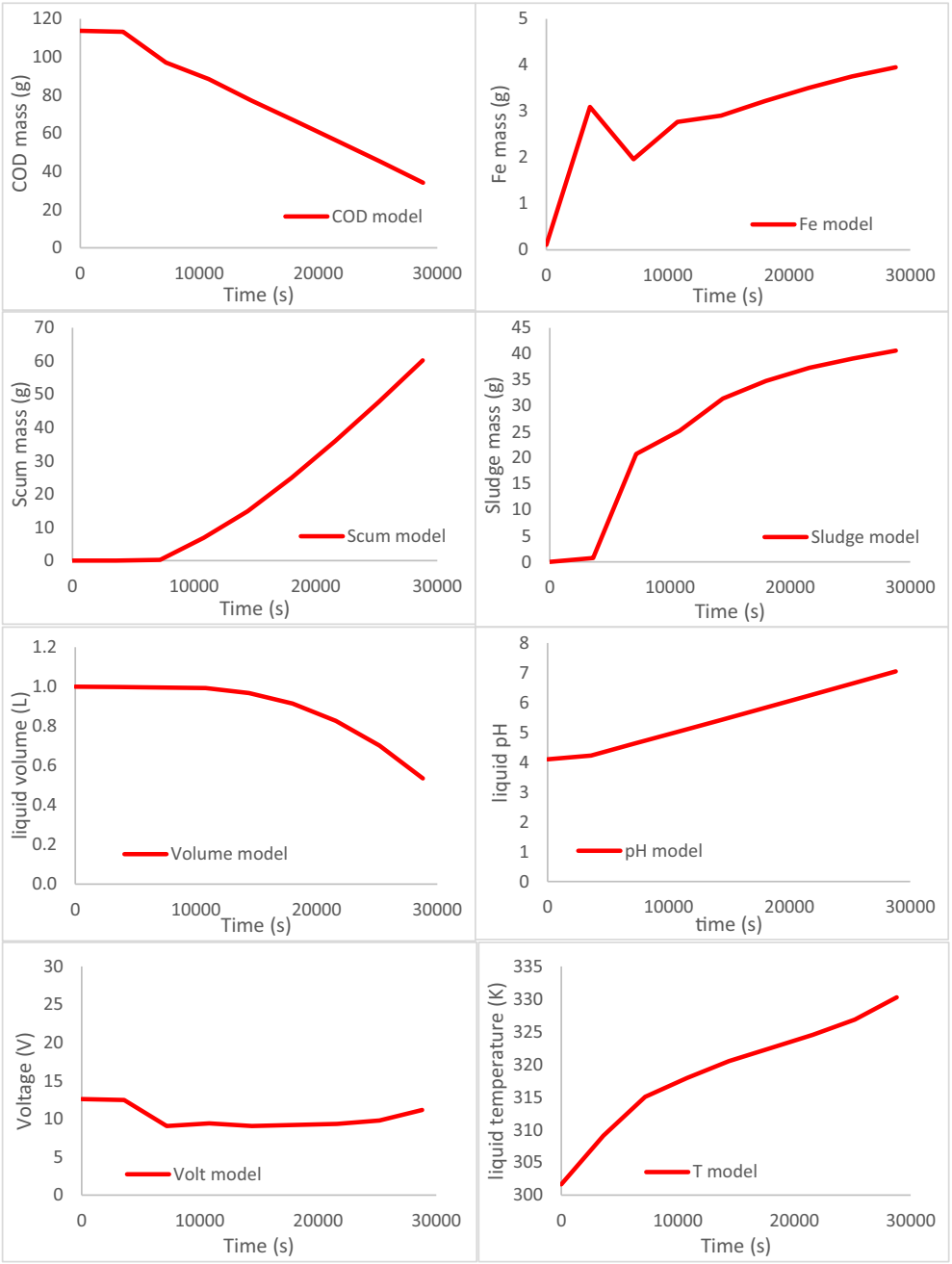

Fig. 8. Prediction of EC process at optimum Re number of 3.82×10^4

and pollutants too short, so the adsorption process was not effective and the floc mass was produced in a little amount. Meanwhile, too high agitation speed broke the H_2 bubbles so the flotation process was low and the scum mass were produced in a little amount.

5.1.3. The liquid volume profiles

The liquid volume decreased during the EC process. A decrease in volume can be caused by (2) the reduction reaction of water and (2) scum production [14]. The rate of the decrease in liquid volume at 250 rpm was faster than that at 0 and 500 rpm (Table 3). Because of the electrical current of 3A applied for all various agitation speeds, the decrease in liquid volume by reduction reaction of water is almost the same for all variables. Therefore, the decrease in liquid volume by the scum production was more dominant than that by the reduction reaction of water. The agitation speed of 250 rpm resulted in more scum mass than the other agitation speeds (Fig. 2), so the rate of the decrease in liquid volume at 250 rpm was higher than that at 0 and 500 rpm.

5.1.4. The liquid pH and temperature profiles

The liquid pH during the EC process is shown in Table 3. The liquid pH increased from the beginning to the end of the process. An increase in liquid pH was caused by the OH^- accumulation in the liquid [13]. At the cathode, the water is reduced to OH^- ion and H_2 gas. The OH^- reacts with Fe^{2+} to form $Fe(OH)_2$. The remaining OH^- in solution was accumulated and then increased the liquid pH [12]. The liquid temperature increased from the beginning to the end of the process (Table 3). The increase in liquid temperature was caused by energy supplied from the electrical current continuously input to the liquid [14].

5.1.5. The electrical voltage profiles

In this study, the electrical current was kept constant at 3 A. Hence, the electrical voltage changed during the EC process because the electrical resistance changed. A correlation between electrical current (I), voltage (V), and resistance (R) is presented in Eq. (37) [14].

$$V = IR \tag{37}$$

Based on Eq. (37), an increase in the R value increased the V value. From the beginning to the middle of the process, the voltage decreased due to the decrease in the electrical resistance. The ions (Fe^{2+} and OH^{-}) in the high amounts at beginning of the process can decrease the electrical resistance. Furthermore, from the middle to the end of the process, the voltage increased. At the time range, the number of ions (Fe^{2+} and OH^{-}) decreased, but the sludge increased, so the electrical resistance increased and the voltage increased too.

5.2. Modeling

The mechanistic model (Table 2) successfully predicted the EC process. The fitting between the experimental data and modeled data were shown in Figs. 3–5. Based on Fig. 6, the mechanistic model can work well with a very high R^2 which was 0.9977–0.9988. Meanwhile, the kinetic constant values (k_a, N, k_v, k_f, k_{pH}, k_{Ri}, k_{Rd}, k_{ht}, k_c) were presented in Table 4. Furthermore, an analysis was conducted to judge which kinetic constants were affected or not affected by the agitation speed (or Re number).

The relative standard deviation (RSD) is usually used in analytical chemistry to express the precision of an assay. The RSD formula is written in Eq. (38).

$$RSD(\%) = \frac{Standard\ Deviation\ (SD)}{Mean} \times 100\% \tag{38}$$

The less the RSD value, the smaller the spread of the data and the higher the precision level. The acceptable value of the RSD value is not >20 % [29,30].

In this study, the RSD is used to judge which kinetic constants are affected or not affected by the agitation speed (or Re number). If the RSD is below 20 %, the kinetic constants are not affected by the agitation speed (or Re number). Table 4 shows the RSD for all kinetic constants. Based on the RSD value, kinetic constants of N, k_v, k_f were affected by Re number because their RSD values are above 20 % in which the value of the kinetic constants spread widely. In other words, the value of the kinetic constants was the function of the Re number. On the opposite side, the RSD value for k_a, k_{pH}, k_{Ri}, k_{Rd}, k_{ht}, k_c was below or equal to 20 %. It means the kinetic values were not affected by the Re number.

5.3. Kinetic analysis

5.3.1. The kinetic constants of k_a and N

Based on Table 4, the kinetic constant of k_a was not affected by the Re number. This kinetic constant presented the adsorption reaction between the coagulant and the COD. The higher the k_a value, the more the Fe^{2+} ions were to be coagulant and contributed to the adsorption reaction. Variation of agitation speeds in the range of 0 to 500 rpm or Re number in the range of 0 to 1.09×10^5 resulted in the not significant k_a values which were 1.06×10^{-4}-1.10×10^{-4} L/(mol.s). It means the amount of Fe^{2+} contributing to the adsorption reaction was almost the same for all various Re numbers. Based on experimental data, the Fe^{2+} contributing in coagulant and then in flocs formation was around 87.09–91.49 % for all various agitation speeds (Re number).

Furthermore, the value of N increased from 6.00 to 6.28 with increasing the Re number from 0 to 5.47×10^4 (Table 4). The kinetic constant of N presented the amount of COD that can be adsorbed by each Fe^{2+} (coagulant). Therefore, increasing the Re number from 0 to 5.47×10^4 successfully increased the ability of each coagulant to adsorb the COD. However, a further increase in the Re number from 5.47×10^4 to 1.09×10^5 decreased the value of N (Table 4). It means that the ability of the coagulant decreased along with an increase in the Re number from 5.47×10^4 to 1.09×10^5. Too high the Re number was not recommended because the adsorption of COD on coagulants was not effective, so the rate of COD mass removal at the Re of 1.09×10^5 was lower than that at the Re of 5.47×10^4. The highest value of N of 6.28 was obtained at Re of 5.47×10^4. Hence, the Re number of 5.47×10^4 (250 rpm) was more effective than the two others.

5.3.2. The kinetic constant of k_f

The sludge resulted from the reaction between the coagulant and the COD. Hence, the higher the N value, the more the flocs can be resulted. Due to the Re of 5.47×10^4 having a higher N value, a higher amount of flocs was resulted at the Re number. Furthermore, the kinetic constant of k_f showed the rate of flotation reaction. It means the higher the k_f value, the faster the flotation reaction occurred. Re number of 5.47×10^4 resulted in a higher k_f value (8.62×10^{-5}/s) than the other Re numbers (3.17×10^{-5} - 8.22×10^{-5}/s) (Table 4). The Re number of 5.47×10^4 resulted in a higher amount of flocs than the two others because it had a higher N value than the two others. The more the flocs mass, the easier the scum was formed.

5.3.3. The kinetic constant of k_v

Based on Table 4, the increase in Re number from 0 to 1.09×10^5 increased the k_v value from 1.22×10^{-6} to 1.98×10^{-6} L/(g.s) (Table 4). The kinetic constant of k_v represent the amount of the liquid volume that can be included in the scum formation. Scum was formed from flocs that were pushed by hydrogen gas bubbles to the surface of the liquid. The high agitation speed can break the big hydrogen bubbles into small hydrogen bubbles. The smaller the hydrogen bubble size, the wider the contact area of the bubbles on the liquid. Therefore, more liquid can be brought by the smaller bubbles. Finally, the liquid included in the scum formation was more at a faster agitation speed (Re number).

5.3.4. The kinetic constant of k_{pH}, k_{Ri}, k_{Rd}, k_{ht}, k_c

The kinetic constant of k_{pH} presented the rate of increase in liquid pH during the EC process. The k_{pH} values were not affected by the Re numbers because the values were almost the same (7.71×10^{-6}–9.12×10^{-6}/s) (Table 4). Furthermore, the kinetic constant of k_{Ri} and k_{Rd} presented the rate of increase and decrease in electrical resistance, respectively. These kinetic constants were not affected by the Re number based on the RSD value of 19–20 %. Moreover, the kinetic constant of k_{ht} and k_c presented the rate of increase and decrease in liquid temperature, respectively. These kinetic constants were also not affected by the Re number based on the RSD value of 4–6 %.

5.4. Advanced mechanistic model as a function of Re number

Based on Table 4, the agitation speed (Re number) affected the kinetic constant values of N, k_v, k_f, but not values of k_a, k_{pH}, k_{Ri}, k_{Rd}, k_{ht}, k_c. Hence, it was important to build correlations between the Re number and the value of N, k_v, k_f and Fig. 7 shows those correlations. The equations of the correlation are shown in Eqs. (39)–(41).

$$N = -4 \times 10^{-10} Re^2 + 3 \times 10^{-5} Re + 6 \tag{39}$$

$$k_v = 1 \times 10^{-16} Re^2 - 5 \times 10^{-12} Re + 1 \times 10^{-6} \tag{40}$$

$$k_f = -1 \times 10^{-14} Re^2 + 6 \times 10^{-10} Re + 8 \times 10^{-5} \tag{41}$$

Furthermore, the mean values of k_a, k_{pH}, k_{Ri}, k_{Rd}, k_{ht}, k_c (Table 4) can be used as the universal values that can predict the EC process with the Re range of 0–1.09×10^5.

The mechanistic model in Table 2 with the kinetic constant values of N, k_v, k_f as a function of Re number (Eqs. (39)–(41)) and the mean value of kinetic constants of k_a, k_{pH}, k_{Ri}, k_{Rd}, k_{ht}, k_c can be used to predict the

EC process at various Re numbers with a range from 0 to 1.09×10^5. The optimization can be conducted to find the optimum Re number which results in the maximum COD mass removal value. Based on an optimization, the best Re number was 3.82×10^4 with a COD mass removal of 70.01 %. The EC process at Re of 3.82×10^4 can be predicted and is shown in Fig. 8.

6. Conclusion

The agitation speed in the EC process was varied to 0, 250, and 500 rpm which can be converted to the Re number of 0, 5.47×10^4, and 1.09×10^5, respectively. After 8 h, the EC process at the Re of 0, 5.47×10^4, and 1.09×10^5 resulted in the COD mass removal of 63.44, 67.62, and 42.27 %, respectively. Meanwhile, the Re of 0, 5.47×10^4, and 1.09×10^5 resulted in a total mass of sludge and scum of 94.56, 99.96, and 70.04 g, respectively. Furthermore, a detailed mechanistic model was successfully built with nine kinetic constants of k_a, N, k_v, k_f, k_{pH}, k_{Ri}, k_{Rd}, k_{ht}, k_c. The mechanistic model was successfully used to simulate the EC process at the agitation speeds with a very high R^2 of 0.9977–0.9988. Based on simulation results, the Re number affected the value of N, k_v, k_f, but not the value of k_a, k_{pH}, k_{Ri}, k_{Rd}, k_{ht}, k_c. Furthermore, the equations expressing the values of N, k_v, k_f as a function of Re number were built. Finally, the optimization was conducted to find the optimum Re number to result in the maximum COD mass removal. The predicted optimum Re was 3.82×10^4 with maximum COD mass removal of 70.01 % or maximum COD concentration removal of 44 %.

Declaration of competing interest

The authors declare that they have no known competing financial interests or personal relationships that could have appeared to influence the work reported in this paper.

Data availability

Data will be made available on request.

Acknowledgements

The authors thank the Chemical Engineering Department, University of Sultan Ageng Tirtayasa for supporting this study and the Chemical Engineering Department, Universitas Gadjah Mada for facilitating this study with excellent laboratories. The authors also thank the LPDP for providing financial support for this study.

References

[1] S. Garcia-Segura, M.M.S.G. Eiband, J.V. de Melo, C.A. Martínez-Huitle, Electrocoagulation and advanced electrocoagulation processes: a general review about the fundamentals, emerging applications and its association with other technologies, J. Electroanal. Chem. 801 (2017) 267–299, https://doi.org/10.1016/J.JELECHEM.2017.07.047.

[2] M.E. Bote, Studies on electrode combination for COD removal from domestic wastewater using electrocoagulation, Heliyon. 7 (2021), e08614, https://doi.org/10.1016/J.HELIYON.2021.E08614.

[3] P. Gautam, S. Kumar, S. Vishwakarma, A. Gautam, Synergistic optimization of electrocoagulation process parameters using response surface methodology for treatment of hazardous waste landfill leachate, Chemosphere 290 (2022), 133255, https://doi.org/10.1016/J.CHEMOSPHERE.2021.133255.

[4] A. Shokri, M.S. Fard, A critical review in electrocoagulation technology applied for oil removal in industrial wastewater, Chemosphere 288 (2022), 132355, https://doi.org/10.1016/J.CHEMOSPHERE.2021.132355.

[5] R. Shankar, L. Singh, P. Mondal, S. Chand, Removal of COD, TOC, and color from pulp and paper industry wastewater through electrocoagulation, Desalin. Water Treat. 52 (2014) 7711–7722, https://doi.org/10.1080/19443994.2013.831782.

[6] A.A. Oladipo, F.S. Mustafa, O.N. Ezugwu, M. Gazi, Efficient removal of antibiotic in single and binary mixture of nickel by electrocoagulation process: hydrogen generation and cost analysis, Chemosphere 300 (2022), 134532, https://doi.org/10.1016/J.CHEMOSPHERE.2022.134532.

[7] P. Asaithambi, R. Govindarajan, M.B. Yesuf, P. Selvakumar, E. Alemayehu, Investigation of direct and alternating current–electrocoagulation process for the treatment of distillery industrial effluent: studies on operating parameters, J. Environ. Chem. Eng. 9 (2021), 104811, https://doi.org/10.1016/J.JECE.2020.104811.

[8] Y. Yang, Y. Li, R. Mao, Y. Shi, S. Lin, M. Qiao, X. Zhao, Removal of phosphate in secondary effluent from municipal wastewater treatment plant by iron and aluminum electrocoagulation: efficiency and mechanism, Sep. Purif. Technol. 286 (2022), 120439, https://doi.org/10.1016/J.SEPPUR.2021.120439.

[9] M. Kobya, E. Senturk, M. Bayramoglu, Treatment of poultry slaughterhouse wastewaters by electrocoagulation, J. Hazard. Mater. 133 (2006) 172–176, https://doi.org/10.1016/J.JHAZMAT.2005.10.007.

[10] Z. Guo, Y. Zhang, H. Jia, J. Guo, X. Meng, J. Wang, Electrochemical methods for landfill leachate treatment: a review on electrocoagulation and electrooxidation, Sci. Total Environ. 806 (2022), 150529, https://doi.org/10.1016/J.SCITOTENV.2021.150529.

[11] E.D. Ongley, Water Quality of the Lower Mekong River, Academic Press, 2009, https://doi.org/10.1016/B978-0-12-374026-7.00012-7.

[12] I. Syaichurrozi, S. Sarto, W.B. Sediawan, M. Hidayat, Effect of current and initial pH on electrocoagulation in treating the distillery spent wash with very high pollutant content, Water 13 (2021) 11, https://doi.org/10.3390/W13010011.

[13] I. Syaichurrozi, S. Sarto, W.B. Sediawan, M. Hidayat, Mechanistic model of electrocoagulation process for treating vinasse waste: effect of initial pH, J. Environ. Chem. Eng. 8 (2020), 103756, https://doi.org/10.1016/J.JECE.2020.103756.

[14] I. Syaichurrozi, S. Sarto, W.B. Sediawan, M. Hidayat, Mechanistic models of electrocoagulation kinetics of pollutant removal in vinasse waste: effect of voltage, J. Water Process Eng. 36 (2020), 101312, https://doi.org/10.1016/J.JWPE.2020.101312.

[15] I. Syaichurrozi, S. Sarto, W.B. Sediawan, M. Hidayat, The new mechanistic model to illustratethe complex phenomena in electrocoagulation process of vinasse, Polish J. Environ. Stud. 30 (2021) 3249–3259, https://doi.org/10.15244/PJOES/130906.

[16] M. Parsaee, M.Kiani Deh Kiani, K. Karimi, A review of biogas production from sugarcane vinasse, Biomass and Bioenergy 122 (2019) 117–125, https://doi.org/10.1016/J.BIOMBIOE.2019.01.034.

[17] S. Bayar, Y.S. Yildiz, A.E. Yilmaz, S. Irdemez, The effect of stirring speed and current density on removal efficiency of poultry slaughterhouse wastewater by electrocoagulation method, Desalination 280 (2011) 103–107, https://doi.org/10.1016/j.desal.2011.06.061.

[18] M. Negarestani, M. Motamedi, A. Kashtiaray, A. Khadir, M. Sillanpää, Simultaneous removal of acetaminophen and ibuprofen from underground water by an electrocoagulation unit: operational parameters and kinetics, Groundw. Sustain. Dev. 11 (2020), 100474, https://doi.org/10.1016/J.GSD.2020.100474.

[19] A. Mohammadi, A. Khadir, R.M.A. Tehrani, Optimization of nitrogen removal from an anaerobic digester effluent by electrocoagulation process, J. Environ. Chem. Eng. 7 (2019), 103195, https://doi.org/10.1016/J.JECE.2019.103195.

[20] D. Lakshmanan, D.A. Clifford, G. Samanta, Ferrous and ferric ion generation during iron electrocoagulation, Environ. Sci. Technol. 43 (2009) 3853–3859, https://doi.org/10.1021/ES8036669/SUPPL_FILE/ES8036669_SI_001.PDF.

[21] M. Ben Sasson, W. Calmano, A. Adin, Iron-oxidation processes in an electroflocculation (electrocoagulation) cell, J. Hazard. Mater. 171 (2009) 704–709, https://doi.org/10.1016/J.JHAZMAT.2009.06.057.

[22] J.F. Pires, G.M.R. Ferreira, K.C. Reis, R.F. Schwan, C.F. Silva, Mixed yeasts inocula for simultaneous production of SCP and treatment of vinasse to reduce soil and fresh water pollution, J. Environ. Manag. 182 (2016) 455–463, https://doi.org/10.1016/J.JENVMAN.2016.08.006.

[23] J.N. Hakizimana, B. Gourich, M. Chafi, Y. Stiriba, C. Vial, P. Drogui, J. Naja, Electrocoagulation process in water treatment: a review of electrocoagulation modeling approaches, Desalination 404 (2017) 1–21, https://doi.org/10.1016/J.DESAL.2016.10.011.

[24] M.F. Ni'am, F. Othman, J. Sohaili, Z. Fauzia, Electrocoagulation technique in enhancing COD and suspended solids removal to improve wastewater quality, Water Sci. Technol. 56 (2007) 47–53, https://doi.org/10.2166/WST.2007.678.

[25] O. Larue, E. Vorobiev, Floc size estimation in iron induced electrocoagulation and coagulation using sedimentation data, Int. J. Miner. Process. 71 (2003) 1–15, https://doi.org/10.1016/S0301-7516(03)00026-7.

[26] M. Vivas-Cortez, A. Fleitas, P.M. Guzmán, J.E. Nápoles, J.J. Rosales, Newton''s law of cooling with generalized conformable derivatives, Symmetry 13 (2021) 1093, https://doi.org/10.3390/SYM13061093.

[27] W. Adamski, M. Szlachta, Water treatment technology : principles and modeling, PRINTPAP Łódź, Wrocław. https://9lib.org/document/7q06x03q-water-treatment-technology-principles-and-modeling.html, 2011 (diakses 14 Februari 2022).

[28] V. Khandegar, A.K. Saroha, Electrochemical treatment of distillery spent wash using aluminum and iron electrodes, Chin.J. Chem. Eng. 20 (2012) 439–443, https://doi.org/10.1016/S1004-9541(11)60204-8.

[29] E.F. Mcfarren, R.J. Lishka, J.H. Parker, Criterion for judging acceptability of analytical methods, Anal. Chem. 42 (2002) 358–365, https://doi.org/10.1021/AC60285A009.

[30] C.M. Riley, T.W. Rosanske, S.R.R. Riley, Specification of Drug Substances and Products: Development and Validation of Analytical Methods, Elsevier Ltd, 2013, https://doi.org/10.1016/C2013-0-00323-4.